

The non-thermal radiation - Cluster Merger Connection

Pasquale Blasi ^a

^a*NASA/Fermilab Theoretical Astrophysics Group,
Fermi National Accelerator Laboratory, Box 500, Batavia, IL 60510-0500*

Abstract

There is compelling evidence that at least some clusters of galaxies are powerful sources of non-thermal radiation. In all cases where this radiation has been detected, a general trend is that high energy densities of cosmic rays and correspondingly low values of the average magnetic field are required in order to have a self-consistent picture of the multiwavelength observations. Mergers of clusters of galaxies might provide large enough cosmic ray injection rates and at the same time provide the mechanism for the heating of the intracluster medium to the observed temperatures. In this paper we analyze critically all the components that play a role in the non-thermal emission of clusters during a merger, with special attention to mergers occurred in the past of the cluster. We outline the consequences of this model for high energy gamma ray observations and for Faraday rotation measurements of the intracluster magnetic field.

1 Introduction

The non-thermal radiation observed in several clusters of galaxies at frequencies varying from the radio (see [1] for a recent review) to the UV to the soft and hard X-rays, is seriously challenging our understanding. In fact, at least for clusters with an extended radio halo (for instance Coma) the existence of a correspondingly diffuse hard X-ray excess was expected, simply on the basis of the inverse compton scattering (ICS) of the same electron population responsible for the radio radiation, the latter being due to synchrotron emission in the intracluster magnetic field. However, after the first positive detection of an hard X-ray excess in Coma [2], a clear problem arose: the combination of the synchrotron plus ICS model for the radio and X-ray emissions suggested a very large cosmic ray energy density and a strength of the intracluster magnetic field much smaller than the lower limits imposed by Faraday rotation measurements [3,4], typically larger than a μG .

Since the main reason for these problems resides in the synchrotron plus ICS model, some attempts have been made to look for alternative interpretations of the hard X-ray excess, in particular invoking the bremsstrahlung emission from a non-thermal tail in the electron distribution, produced by stochastic acceleration [5–7]. The X-ray spectra can be fitted by this model without requiring small magnetic fields, although large injection rates of MHD waves are needed (compatible with the expectations in a merger of two clusters of galaxies).

As mentioned above, some clusters also show a UV to soft X-ray excess, which could also be the result of ICS of low energy electrons, but very large cosmic ray energy densities are required in this case as well, so that some authors are now reconsidering the possibility of a thermal origin [8,9].

In [10] it was shown that the overall energy density in cosmic rays in a cluster is severely constrained by the upper limits on the gamma ray emission of the cluster, and some new observational tests of 100 GeV - 1 TeV gamma ray astronomy were proposed, aimed to weigh the non-thermal content of clusters of galaxies.

A serious effort to find powerful sources of cosmic rays in clusters was done in [11] (see also references therein): ordinary galaxies, radio galaxies, accretion shocks and a possible bright phase in the galaxy evolution were investigated, but the resulting energy densities found there fall short of the ones required to explain the multiwavelength observations by a factor 10-100. An analysis of the energetic requirements for the radiating electrons in clusters was presented in [12] while the corresponding proton component was studied in detail in [13,11,14]. More recently an increasing interest has been shown for mergers of clusters of galaxies as events responsible for the heating of the cluster, through the formation and propagation of strong shocks in the intracluster medium (see for instance [15] and references therein). The basic question that we want to address in this paper is whether these merger related shocks can accelerate particles by the first order Fermi mechanism (for a review on Fermi acceleration see [16]), to the level required to explain the observations at different wavelengths without invoking anything but the synchrotron emission and ICS and without violating the gamma ray limits, when available. Since most of the previous calculations concentrated either on the primary electrons (neglecting electrons produced as secondaries of cosmic ray interactions) or on the secondary electrons (without considering the electrons directly accelerated at the shocks), in this paper we will try to include all these components in a self-consistent way.

The aim of this paper is to draw some general conclusions, as much independent as possible of a specific cluster, though we also apply our results to the case of Coma, as an example.

The paper is structured as follows: in section 2, we describe our current understanding of the merger between two clusters of galaxies; in section 3 we describe our approach to the transport of the electronic and hadronic components; in section 4 we summarize the radiation process relevant for the production of radio, X, UV and gamma rays. In section 5 we study the conditions that result in the observed non-thermal phenomena; in section 6 we apply our calculations to the case of the Coma cluster. Our discussion and conclusions are presented in section 7.

2 Clusters mergers: thermal heating and particle acceleration

Mergers between clusters of galaxies are among the most energetic phenomena in the universe. During the merger event the formation of strong shocks is practically unavoidable and a substantial fraction of the gravitational energy is released in the form of heating of the intracluster medium. The overall energy in the event can be estimated as

$$E_{merger} \sim \frac{GM_1M_2}{d} \sim 1.4 \times 10^{64} \left(\frac{M}{5 \times 10^{14} M_\odot} \right)^2 \left(\frac{d}{1.5 \text{ Mpc}} \right)^{-1} \text{ ergs}, \quad (1)$$

where on the left-hand side $M_{1,2}$ represent the total masses of the two clusters, and on the right-hand side they have been normalized to the same value of $5 \times 10^{14} M_\odot$, typical of average clusters. d is a fiducial value for the spatial scale where the dissipation through collisionless shocks is likely to occur, taken here to be ~ 1.5 Mpc. It is easy to verify that E_{merger} is roughly comparable with the total thermal energy in the intracluster medium (ICM) of a rich cluster, which justifies the idea that mergers may play a role in the heating of the ICM.

The process of heating of the ICM during merger events has been studied in detail in numerical simulations (e.g. [17–21]). These studies suggest that the main channel of energy dissipation during a merger is associated with the heating of the gas, leaving a few tens of percent available for additional processes as particle acceleration to suprathermal energies. This is consistent with the usual picture of shock acceleration at supernova remnants, where 1 – 10% of the kinetic energy of the plasma is transformed into energy of non-thermal particles. The numerical simulations also provide valuable information about the fluid dynamics of these shocks: for instance typical velocities of $v \gtrsim 10^8$ cm/s and typical compression factors $r \approx 3 - 4$ are achieved [22]. The typical duration of a merger event is therefore $t_{merger} \sim d/v \sim 10^9$ yrs. Consequently the total rate of energy release during the merger is $L_{merger} \sim E_{merger}/t_{merger} \sim 4 \times 10^{47} \left(\frac{M}{5 \times 10^{14} M_\odot} \right)^2 \left(\frac{d}{1.5 \text{ Mpc}} \right)^{-1}$ erg/s.

Some fraction of this energy (left as a parameter) will be converted to kinetic energy of suprathermal particles, due to Fermi acceleration. In the following we estimate the maximum energy of electrons and protons accelerated at the merger shocks and their spectrum. The acceleration time can be written as follows:

$$\tau_{acc}(E) = \frac{3}{u_1 - u_2} D(E) \left[\frac{1}{u_1} + \frac{1}{u_2} \right] = \frac{3D(E)}{v^2} \frac{r(r+1)}{r-1}, \quad (2)$$

valid for any choice of the diffusion coefficient. Here u_1 and u_2 are the upstream and downstream velocities of the fluid and $r = u_1/u_2$ is the compression factor.

We consider two possibilities for the diffusion coefficient $D(E)$. First we use the expression proposed in [23]:

$$D(E) = 2.3 \times 10^{29} B_\mu^{-1/3} L_{20}^{2/3} E(\text{GeV})^{1/3} \text{cm}^2/\text{s}, \quad (3)$$

where B_μ is the magnetic field in microgauss and L_{20} is the largest scale in the magnetic field power spectrum in units of 20 kpc. Here we assumed that the magnetic field is described by a Kolmogorov power spectrum.

In this case the acceleration time becomes:

$$\tau_{acc}(E) \approx 6.9 \times 10^{13} B_\mu^{-1/3} L_{20}^{2/3} E(\text{GeV})^{1/3} v_8^{-2} g(r) \quad \text{s}, \quad (4)$$

where $v_8 = \frac{v}{10^8 \text{cm/s}}$ and $g(r) = r(r+1)/(r-1)$ and $v = u_1$.

For electrons, if the average magnetic field is less than $\sim 3\mu\text{G}$, the energy losses are dominated by ICS off the microwave background, with a loss time $\tau_{loss} \approx 4 \times 10^{16}/E$ s, where E is in GeV. The maximum energy of accelerated electrons is obtained requiring $\tau_{acc} < \tau_{loss}$:

$$E_{max}^e \approx 118 L_{20}^{-1/2} B_\mu^{1/4} v_8^{3/2} g(r)^{-3/4} \text{GeV}, \quad (5)$$

The compression ratio r and the velocity v_8 are not independent, since

$$r = \frac{\frac{8}{3} \mathcal{M}^2}{\frac{2}{3} \mathcal{M}^2 + 2}, \quad (6)$$

valid for an ideal monoatomic gas. Here \mathcal{M} is the Mach number of the unshocked gas, moving with speed v_8 .

For protons, energy losses are not relevant and the maximum energy is clearly determined by the finite time duration of the merger event. Therefore the

maximum energy for protons will be defined by the condition $\tau_{acc} < t_{merger}$, which gives

$$E_{max}^p \approx 9 \times 10^7 L_{20}^{-2} B_\mu v_8^6 g(r)^{-1/2} \text{ GeV}. \quad (7)$$

The second possibility for the diffusion coefficient is a Bohm diffusion, well motivated for the case of strong turbulence. In this case:

$$D(E) = 3.3 \times 10^{22} E/B_\mu \text{ cm}^2/s. \quad (8)$$

This represents the smallest diffusion coefficient (although it can be further decreased in the case of perpendicular shocks [35]) and implies considerably larger maximum energies than the ones estimated above. For electrons we obtain:

$$E_{max}^e \approx 6.3 \times 10^4 B_\mu^{1/2} v_8 g(r)^{-1/2} \text{ GeV}, \quad (9)$$

while for protons

$$E_{max}^p \approx 3 \times 10^9 B_\mu v_8^2 g(r)^{-1} \text{ GeV}. \quad (10)$$

If E_{max}^p becomes larger than $\sim 10^{10}$ GeV energy losses due to pair production and photopion production on the photons of the microwave background become important and limit the maximum energy to less than a few 10^{10} GeV.

Some final comments on the spectrum of accelerated particles are in order. Standard shock acceleration theory predicts that the suprathermal particles generated by the Fermi process have a power law spectrum in momentum, $Q(p)dp \propto p^{-\sigma} dp$ where $\sigma = (r + 2)/(r - 1)$. As mentioned above, numerical simulations predict compression ratios in the range $r = 3-4$, which correspond to $\sigma = 2 - 2.5$ [22].

The classical dilemma of normalizing the electrons and protons spectra exists here as well as for the much better studied case of supernova remnants. It is usually assumed (motivated by observations of the relative abundance in the Galaxy) that at $E \sim 1$ GeV the protons overcome the electron number density by a factor 10-100. More conservatively we introduce a parameter $\xi < 1$ representing the ratio of the injection spectra of electrons and protons (this fraction is later changed by propagation effects).

Theoretically, the motivations for having a small e/p ratio are in the microscopic processes responsible for the acceleration: protons resonate with Alfvén waves on a very wide range of momenta, and it is therefore not too difficult to

extract them from the thermal distribution and inject them into the acceleration region. For electrons this is much harder. Low energy electrons, close to the thermal distribution, do not interact with Alfvén waves and some other modes need to be excited (for instance whistlers) and sustained against the strong damping. If these wave modes are excited they might be responsible for the injection of a fraction of the thermal electrons into the acceleration region. A more detailed discussion of the electron injection at non relativistic shocks can be found in [24,25] and references therein.

There is a even more general reason for the minor efficiency of electron acceleration: a particle is accelerated at the shock only if it can “feel” the shock, which means that its Larmor radius must be larger than the thickness of the shock. The latter quantity is determined by the Larmor radius of thermal protons (see [26,27] and references therein), therefore, for a proton temperature of ~ 8 keV, only electrons of energy larger than $\sim 5 - 10$ MeV can be injected in the acceleration box (note that this value is much larger than the typical electron temperature in the ICM). In the following we will adopt the value of 5 MeV as a low energy cutoff in the injection spectrum of electrons. Although the details of the electron injection are still not completely clear, it seems quite plausible that shock acceleration works more efficiently for the proton component rather than for the electrons. It is extremely important to keep in mind a fundamental difference between electrons and protons in clusters of galaxies: while electrons suffer severe energy losses and they can only trace the recent activity of the cluster, protons are stored on cosmological time scales [11,13] without appreciable losses, being therefore able to produce secondary products (electrons, gamma rays and neutrinos) at any time. It is therefore of great importance to include the hadronic component in any calculation of non-thermal phenomena in clusters of galaxies.

3 The transport of non-thermal particles

The passage of the shock through the cluster heats the gas and possibly accelerates a fraction of electrons and protons to suprathermal energies. The injection spectra are modified by the propagation (diffusion) in the intracluster magnetic field and by energy losses, therefore the electron and proton spectra at each time must be calculated by solving a transport equation, in the form:

$$\frac{\partial n_j(E_j, r, t)}{\partial t} = \frac{1}{r^2} \frac{\partial}{\partial r} \left[r^2 D_j(r, E_j) \frac{\partial n(E_j, r, t)}{\partial r} \right] + \frac{\partial}{\partial E_j} [b_j(r, E_j) n_j(E_j, r, t)] + Q_j(E_j, r, t), \quad (11)$$

where the index j labels protons and electrons, D is the diffusion coefficient, in general dependent on energy and distance, b_j is the total rate of energy losses, Q_j is the rate of injection of particles, and finally n_j is the spectrum of the j -th component resulting from diffusion and losses. We are assuming here that the cluster has a spherical symmetry, so that the spatial dependence is all contained in the radial coordinate r . For electrons, the Coulomb, bremsstrahlung, synchrotron and inverse Compton scattering energy losses have been included, while for protons the only relevant loss channel is the pp scattering.

A discussion of the role of the diffusion coefficient is in order: in section 2, two possibilities were considered and the results for the maximum energy of accelerated electrons and protons were very different, as expected. Such large uncertainties in the diffusion coefficient do not affect the solution of eq. (11). The time evolution of the electron component (both primary and secondary) is largely dominated by the fast energy losses, so that the use of eq. (3) or of eq. (8) for the diffusion coefficient makes no difference (in other words, the first term on the left hand side of eq. (11) is small). For the proton component the situation is different, because energy losses are very weak. However, the diffusion times out of the cluster are large, and indeed larger than the age of the cluster, for the energies that we are interested in. This phenomenon of confinement of cosmic rays, was widely discussed in [11], where the concept of clusters of galaxies as “storage rooms” for cosmic rays was first introduced. It was showed there that the spectra of secondaries (electrons, gamma rays, neutrinos) depend only on the properties of the injection spectrum of cosmic rays, and are not affected by the details of the diffusion.

The injection of electrons at the shock is assumed to be a power law in momentum $Q_e(p) = f(r)p^{-\sigma}$, where the function $f(r)$ is taken to be proportional to the local density profile in the cluster, which can be written as:

$$n_{gas}(r) = \frac{n_0}{\left[1 + \left(\frac{r}{r_c}\right)^2\right]^{\frac{3}{2}\beta}}. \quad (12)$$

Here n_0 is the density in the inner core, r_c is the core radius, and β is a phenomenological parameter (see [28] for a review). The normalization constant in the injection spectrum of electrons, $Q_e(p)$, is chosen in order to fit the data.

For the protons the injection spectrum is also a power law in momentum with the same radial dependence, but the absolute normalization is parametrized in terms of the ratio ξ of the injection rate of electrons and protons.

Once the spectrum of protons is calculated by solving eq. (11) for the proton component, the injection spectra of secondary electrons generated by the

decay of charged pions is completely determined. For secondary electrons the injection rate Q_e is

$$Q_e(E_e, r) = \frac{m_\pi^2}{m_\pi^2 - m_\mu^2} n_{gas}(r) c.$$

$$\int_{E_e}^{E_p^{max}} dE_\mu \int_{E_\pi^{min}}^{E_\pi^{max}} \frac{dE_\pi}{E_\pi} \int_{E_{th}(E_\pi)}^{E_p^{max}} dE_p G_\pi(E_\pi, E_p) F_e(E_e, E_\mu, E_\pi) n_p(E_p, r), \quad (13)$$

where E_p^{max} is the maximum proton energy (note that our calculations are insensitive to the exact value of E_p^{max}), $E_{th}(E_\pi)$ is the threshold energy for the production of pions with energy E_π and we put

$$E_\pi^{min} = \frac{2E_\mu}{(1+\beta) + \delta(1-\beta)}; \quad E_\pi^{max} = \min \left\{ E_p^{max}, \frac{2E_\mu}{(1-\beta) + \delta(1+\beta)} \right\},$$

where $\delta = m_\pi^2/m_\mu^2$ and β is the velocity of muons in units of the light speed. The quantity $n_p(E_p, r)$ is the CR spectrum at distance r from the source, as given by eq. (11).

The interactions are described by the functions $G_\pi(E_\pi, E_p)$ (the differential cross section for pions with energy E_π produced in a CR interaction at energy E_p in the laboratory frame) and $F_e(E_e, E_\mu, E_\pi)$ (the spectrum of electrons in the decay of a muon of energy E_μ produced in the decay of a pion with energy E_π). The electron spectrum is given by the following expression:

$$F_e(E_e, E_\mu, E_\pi) = \frac{1}{\beta E_\mu} \times \left. \begin{aligned} & \left\{ \begin{aligned} & 2 \left(\frac{5}{6} - \frac{3}{2} \lambda^2 + \frac{2}{3} \lambda^3 \right) - P_\mu \frac{2}{\beta} \left[\frac{1}{6} - \left(\beta + \frac{1}{2} \right) \lambda^2 + \left(\beta + \frac{1}{3} \right) \lambda^3 \right] & \text{if } \frac{1-\beta}{1+\beta} \leq \lambda \leq 1, \\ & \frac{4\lambda^2\beta}{(1-\beta)^2} \left[3 - \frac{2}{3} \lambda \left(\frac{3+\beta^2}{1-\beta} \right) \right] - \\ & \frac{4P_\mu}{1-\beta} \left\{ \lambda^2(1+\beta) - \left[\frac{1}{2} + \lambda(1+\beta) \right] \frac{2\lambda^2}{1-\beta} + \frac{2\lambda^3(\beta^2+3)}{3(1-\beta)^2} \right\} & \text{if } 0 \leq \lambda \leq \frac{1-\beta}{1+\beta}, \end{aligned} \right\} \end{aligned} \right\} \quad (14)$$

where we put

$$P_\mu = P_\mu(E_\pi, E_\mu) = \frac{1}{\beta} \left[\frac{2E_\pi\delta}{E_\mu(1-\delta)} - \frac{1+\delta}{1-\delta} \right], \quad (15)$$

and $\lambda = E_e/E_\mu$. The above expression for F_e takes into account that the muons produced from the decay of pions are fully polarized (this is the reason why the pion energy E_π appears in the expression for the electron spectrum from the muon decay).

Determining the pion distribution in the low energy region (pion energies close to the mass of the pions) is not trivial. A satisfactory approach to the low energy pion production was proposed in [29,30] and recently reviewed in [31] in the context of the *isobaric model*. The detailed and lengthy expressions for G_π that we used are reported and discussed in details in [31] (see their Appendix). Thus, following [31], we use here their model for collisions at $E_p \lesssim 3$ GeV. For $E_p \gtrsim 7$ GeV we use the scaling approximation which can be formalized writing the differential cross section for pion production as

$$d\sigma/dE_\pi = (\sigma_0/E_\pi)f_{\pi^\pm}(x), \quad (16)$$

where $\sigma_0 = 3.2 \cdot 10^{-26} \text{ cm}^2$, $x = E_\pi/E_p$. The scaling function $f_{\pi^\pm}(x)$ is given by

$$f_{\pi^\pm}(x) = 1.34(1-x)^{3.5} + e^{-18x}. \quad (17)$$

In this case the function G_π coincides with the definition of differential cross section given in eq. (16).

From the discussion above, it is clear that in the case of secondary electrons the transport equations for protons and secondary electrons are coupled.

In the following sections we will solve the transport equations for the different components using some *fiducial* values for the basic parameters for the cluster merger, and for different possibilities for the time evolution of the merger event.

4 Non-thermal radiations

In this section we briefly summarize the mathematical basis for the calculation of the radio, UV, X-ray and gamma ray spectra. Four processes are involved in the production of the radiation: *a)* synchrotron emission; *b)* inverse Compton scattering, *c)* pion production and decay, and *d)* bremsstrahlung of primary and secondary electrons. We discuss them separately.

4.1 Synchrotron emission and radio radiation

High energy electrons produce radio radiation in $\sim \mu G$ magnetic fields by synchrotron emission. The energy generated per unit time, per unit volume,

per unit frequency ν is given by [32]

$$\mathcal{L}(\nu) = \frac{3^{1/2}e^3B}{m_e c^2} \int n(\gamma, r, t) \mathcal{R}(x) d\gamma, \quad (18)$$

where e and m_e are the electron charge and mass respectively, B is the magnetic field, c is the speed of light and n_e is the solution of the transport equation for electrons (primaries or secondaries) with kinetic energy $m_e c^2(\gamma - 1)$ at the position at distance r from the cluster's center at the time t . The function $\mathcal{R}(x)$ is defined as

$$\mathcal{R}(x) = 2x^2 \left\{ K_{4/3}(x) K_{1/3}(x) - \frac{3}{5} x \left[K_{4/3}^2(x) - K_{1/3}^2(x) \right] \right\} \quad (19)$$

and the K_y 's are modified Bessel functions. The variable x is function of γ through $x = \nu/(3\gamma^2\nu_c)$, where the critical frequency is $\nu_c = eB/(2\pi m_e c)$.

4.2 Inverse Compton Scattering (ICS)

The electrons of relevance in clusters of galaxies produce photons by ICS off the CMB background in a wide range of accessible frequencies, from UV to soft X-rays to hard X-rays and gamma rays.

The particle number density per unit volume, per unit time, per unit photon energy E_{ph} at distance r from the cluster's center is given by

$$\mathcal{Q}_{ph}(E_{ph}) = \frac{12\pi\sigma_T}{hE_{ph}} \int_1^\infty d\gamma n_e(\gamma, r, t) \int_0^1 dx \mathcal{G}(x) \mathcal{J}\left(\frac{E_{ph}}{4\gamma^2 h x}\right), \quad (20)$$

where σ_T is the Thomson cross section, $\mathcal{G}(x) = 1 + x + 2x \ln x - 2x^2$ and

$$\mathcal{J}(\tilde{\nu}) = \frac{2h\tilde{\nu}^3}{c^2} \frac{1}{\exp(h\tilde{\nu}/(kT_{CMB})) - 1} \quad (21)$$

is the brightness of the CMB background at temperature T_{CMB} .

4.3 Neutral pion production and decay

Gamma rays are produced by the decay of neutral pions ($\pi^0 \rightarrow \gamma\gamma$) generated in pp inelastic interactions. This channel usually provides an important contribution to the gamma ray fluxes above ~ 100 MeV.

The emissivity in gamma rays at distance r and energy E_γ is given by

$$j_\gamma^{\pi^0}(E_\gamma, r) = 2n_H(r)c \int_{E_\pi^{\min}(E_\gamma)}^{E_p^{\max}} dE_\pi \int_{E_{th}(E_\pi)}^{E_p^{\max}} dE_p G_{\pi^0}(E_\pi, E_p) \frac{n_p(E_p, r)}{(E_\pi^2 - m_\pi^2)^{1/2}}, \quad (22)$$

where $E_\pi^{\min}(E_\gamma) = E_\gamma + m_{\pi^0}^2/(4E_\gamma)$. We refer to [31] for the expression of $G_{\pi^0}(E_\pi, E_p)$ in the low energy collisions ($E \leq 3$ GeV), while we use the scaling approach given in eqs. (16) and (17) for $E_p > 7$ GeV, with $f_{\pi^0} = (1/2)f_{\pi^\pm}$.

4.4 Bremsstrahlung

The flux of gamma rays due to bremsstrahlung of primary and secondary electrons is given by

$$j_\gamma^{\text{brem}}(E_\gamma, r) = n_{gas}(r)c \int_{E_\gamma}^{E_p^{\max}} dE_e n_e(E_e, r) \frac{d\sigma}{dE_\gamma}(E_e, E_\gamma), \quad (23)$$

where the differential cross section can be approximated as

$$\frac{d\sigma}{dE_\gamma}(E_e, E_\gamma) = 2.6 \cdot 10^{-26} / E_\gamma. \quad (24)$$

5 The non-thermal side of mergers

Mergers are able to heat the ICM to the observed temperature through the formation of collisionless shocks. In the same process, some fraction of the thermal particles acquires a suprathermal energy distribution, by first order Fermi acceleration at the same shocks, so that relativistic particles are likely to be generated during the merger. In this section we study the non-thermal appearance of a cluster for different scenarios of a merger.

Since it is not our purpose to study a specific cluster in detail, we will choose a set of fiducial values for the parameters and use those values in our calculations in order to derive some general trends. The dependence of the values of the parameters will be discussed. The total merger luminosity is taken from eq. (1), the magnetic field is taken to be $B = 0.15\mu G$, but the effect of higher fields is studied too. We emphasize the fact that observations force to use these low fields if the X-ray emission is interpreted as ICS. Therefore one must either believe the results of Faraday rotation measurements (larger fields) and

look for alternative interpretation of the hard X-ray excess or have a good reason to discard the results of Faraday rotation measurements and maintain an ICS interpretation for the hard X-ray excess. Indeed it is quite simple to understand this effect: both the radio and ICS fluxes depend linearly on the energy injection rate in the form of electrons, but the former scales with the magnetic field as $B^{1+\gamma/2}$, where γ is the power index of the electron injection spectrum. Therefore, at fixed X-ray (ICS) flux, the radio flux increases very fast with increasing B . For instance for a magnetic field of $1\mu G$ the radio flux would increase by a factor ~ 60 in comparison to the case $B = 0.15\mu G$ (we use here $\gamma = 2.32$). This can be seen in another way: if the radio flux is explained in terms of a μG magnetic field, then the X-ray (ICS) flux will be ~ 60 times smaller than for the case $B = 0.15\mu G$. If $B = 5\mu G$ the factor 60 becomes ~ 2000 .

For clusters which are experiencing a current merger, the non-thermal activity strongly depends on the stage at which the merger is observed. In these cases there are usually strong signatures that particle acceleration is occurring (see the case of A3667 [33]), and they could be used as a testing facility for the ideas presented in this paper. However they represent a subsample of the clusters which show non-thermal activity.

The interesting and most likely case is that of a merger occurred in the past, since most or all of the clusters are supposed to have had at least one merger during their lifetime. It is easy to understand that the results will depend on the time from the merger, when compared with the cooling time of high energy electrons. After $\sim 10^9$ yrs the high energy electrons responsible for the radio and hard X-ray emissions will have cooled through ICS and synchrotron emission, so that the observed spectra will have no radio and hard X-ray emission or have a very weak one. On the other hand electrons will have piled up at low energy, providing a bulk of potentially powerful UV and soft X-ray emitters. Cluster mergers which occurred $\sim 10^9$ years ago will be on the boundary and might or might not show high energy non-thermal emission. These conclusions are based on the primary electrons only, and have also been derived in some different form in [32]. A crucial question is what happens to the hadronic component. In fact, protons do not lose energy in appreciable way on the time scales we are interested in [11,34,23]. Therefore, even if they have been injected in the cluster during a merger in the very past, they are still efficient in generating secondary electrons and high energy radiation at present.

This is a very solid conclusion: if all clusters have experienced a powerful merger at some point of their lifetime, then all of them should have to some extent non-thermal activity, because the proton-induced electron spectra cannot be depleted by energy losses. In other words the secondary electron injection is continuous even if the proton injection occurred in the past of the cluster.

The detectability of this radiation depends on conditions which are specific of the single clusters.

Here we formally calculate the contribution of primary and secondary electrons for different times elapsed from the last merger and show more rigorously what stated above.

The technique used in the calculations is the one illustrated in the previous sections: we inject an electron and proton component, both having a spectrum modelled as a power law in momentum and such that the ratio of the two spectra at injection is given by the parameter ξ (since the spectra are both power laws in momentum this ratio is kept at all momenta). Some comments are required about the total energy content of the electron and proton components: the total energy density injected per unit time in the component i (i = protons, electrons) is

$$E_i = \int_{p_{min}} dp q_0 p^{-\gamma} \epsilon(p), \quad (25)$$

where we wrote both electron and proton spectra in the form $q_{0,e/p} p_{e/p}^{-\gamma}$. For the purpose of an order of magnitude estimate let us assume that the energy $\epsilon(p)$ of a particle with momentum p can be approximated by $p^2/(2m)$ for $p < m$ and by p for $p > m$. In this case it is easy to show that the ratio of energy injections is

$$\frac{E_e}{E_p} \approx \frac{2\xi(3-\gamma)}{4-\gamma} \left(\frac{p_e^{min}}{m_p} \right)^{-\gamma+2}. \quad (26)$$

For the value $\gamma = 2.32$ that we use here (correspondent to $r = 3.27$, compatible with the values found in numerical simulations), and for $p_e^{min} \approx 5$ MeV, obtained above, we obtain $E_e/E_p \approx 4.3\xi$. In other words, if the number density in protons is larger at fixed p by a factor $1/\xi = 10$ (100), the correspondent energy injection rate in protons is a factor 2.3 (23) larger than the energy injection rate in electrons. The correspondent ratio of the rate of injections of particles is $Q_e/Q_p \approx \xi(p_e^{min}/p_p^{min})^{-\gamma+1}$. If we take the minimum kinetic energy of the protons to be ~ 20 keV, and $\gamma = 2.32$ we have $Q_e/Q_p \approx 1.3\xi = 0.13$ (0.013) for $\xi = 0.1$ (0.01).

Both injections are assumed to occur in a way proportional to the local gas density in the ICM. There is a theoretical justification for this: if the only discrimination between a particle that can be accelerated and one that cannot is in the particle energy, and if we assume that the temperature of the cluster is the same at all points, then the fraction of particles energized at the shock must be simply proportional to the local gas density. This simple picture

might be modified because the injection of particles in the acceleration region is thought to occur through resonant scattering with waves, and these waves might be damped more efficiently in the denser regions of the cluster.

For the protons, the rate of secondary electrons is consistently calculated and used in the transport equation to calculate their effective local spectrum at each time. A very important point must be noticed: after the proton injection has stopped (the merger is over) the rate of production of secondary electrons does not change with time, because diffusion is too slow to allow the proton escape from the cluster, and the energy losses of protons do not affect their spectrum. By all means the protons work as a continuous source of “new” electrons in the cluster, even if the process that generated them is no longer operating.

Our results are summarized in Figs. 1 and 2 showing the radio emission and the UV plus X-ray emission of the cluster, for a typical distance of 100 Mpc (the results can be easily rescaled to an arbitrary distance). In Fig. 1 the dashed thin lines represent the radio emission from the primary electron component 0, 5×10^8 and 10^9 yrs after the injection of new particles is finished (as indicated on the plot). These lines are obtained by adopting a diffusion coefficient as in eq. (3) with $v_8 \approx 4.8$ and $L_{20} = 25$ (500 kpc). The thick dashed line represents the radio flux from primary electrons at $t = 0$ in the case of Bohm diffusion [eq. (8)]. It can be clearly seen that only the tail of the radio spectrum is affected by the choice of a different diffusion coefficient (because in this second case the maximum energy of the primary electrons is larger) while the lower frequency spectrum remains almost unaltered (within 10 – 20%), although the two diffusion coefficients are very different. For the curves describing the radio emission at later times, there is no difference as a result of a different choice of the diffusion coefficient. The solid lines represent the radio emission from secondary electrons for the indicated values of ξ . Due to confinement of the primary cosmic rays, these curves are not affected by the choice of the diffusion picture [11]. All the curves mentioned above are obtained for a magnetic field of $0.15\mu G$, but it is important to show the effect of larger fields. As a reference, we plotted as a dash-dotted curve the radio flux for a magnetic field of $1\mu G$. We find that the rate of injection of electrons must be ~ 60 times smaller than before to generate the same radio emission as for the case $B = 0.15\mu G$. This has important consequences for the X-ray fluxes (see below).

It is immediately clear that already after 5×10^8 yrs the radio emission is limited to frequencies less than ~ 30 MHz, not easily accessible to observations, and after 10^9 yrs, the emission is negligible above ~ 5 MHz. There is no way that primary electrons can produce a persistent radio emission up to a few GHz (as in the case of Coma) if the merger event ended more than ~ 20 million years ago. On the other hand the radio emission due to secondary elec-

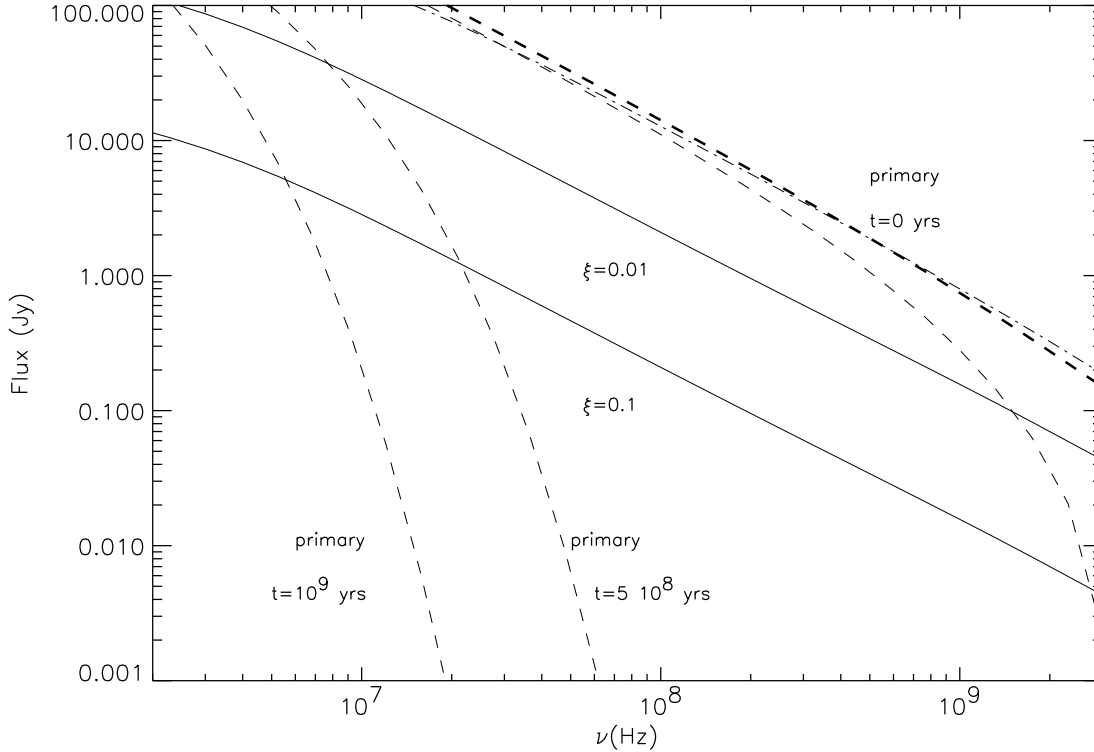


Fig. 1. Radio fluxes from a cluster at 100 Mpc distance. The three dashed thin lines refer to primary electrons at different times after the merger, as indicated. The solid lines are the contributions of secondary electrons for two values of ξ . The dashed thick line is the radio flux from primary electrons at $t = 0$ in case of Bohm diffusion. The dash-dotted line is the synchrotron emission from primary electrons at $t = 0$ in the case $B = 1\mu G$.

trons is irreducible. It persists in the cluster even if the merger occurred at the beginning of the cluster history and it is appreciable even for the conservative value $\xi = 0.1$. The solid curves in Fig. 1 remain unchanged with time, after the end of the merger event.

In Fig. 2 a similar situation is illustrated for the range of energies between 100 eV and 100 keV. The thick solid curves represent the bremsstrahlung emission of a gas of thermal electrons at 8 keV and 4 keV temperature, as indicated. The dashed lines represent the contribution due to ICS of the primary electrons off the photons of the cosmic microwave background, for three different times after the end of the merger. It is possible to see that the X-ray excess at $E_X > 30$ keV (10 keV) is basically negligible for times larger than $\sim 10^9$ years after the merger for a temperature of 8 keV (4 keV). Clearly the non-thermal fluxes are more prominent in the lower temperature case.

As for Fig. 1, the dash-dotted line represents the X-ray flux from primary electrons for a magnetic field of $1\mu G$, immediately after the end of the merger

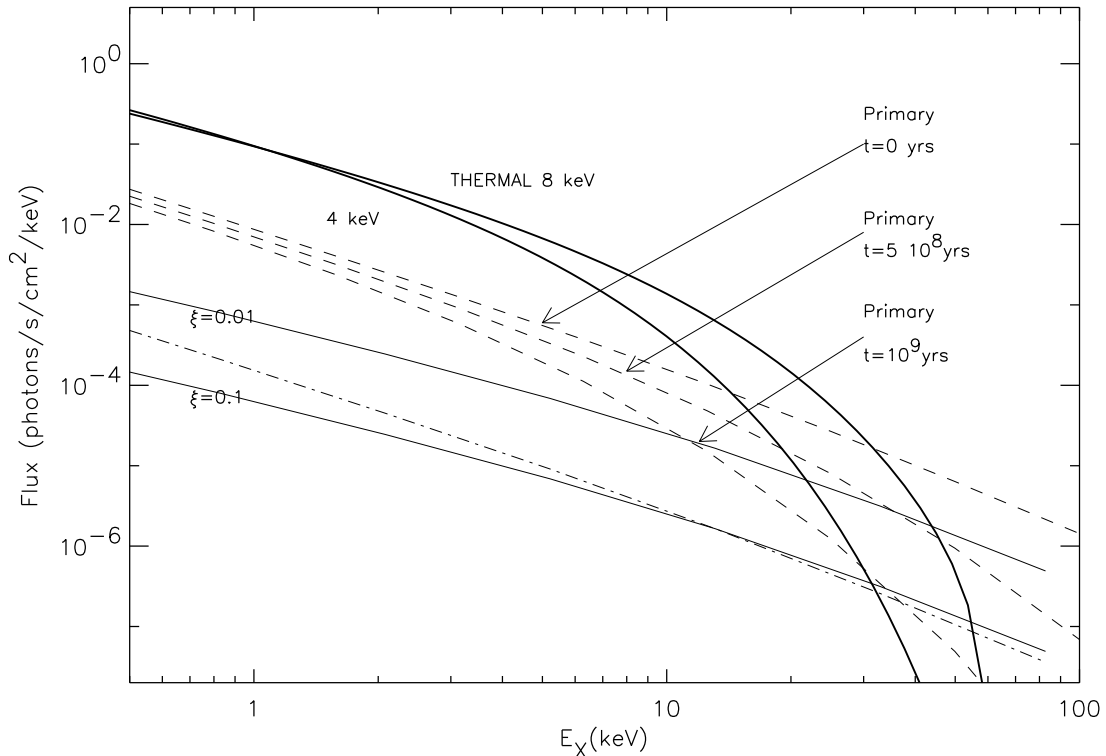


Fig. 2. X-ray fluxes from a cluster at 100 Mpc distance. The thick solid lines are the thermal bremsstrahlung emission of the thermal gas at a temperature of 8 KeV and 4 keV. The other curves are the ICS contribution of non-thermal electrons (labelled as in Fig. 1). The dash-dotted line refers to the case $B = 1\mu G$, to emphasize the fact that X-ray fluxes are suppressed for high magnetic fields.

event. We can clearly see that the X-ray flux in this case is about ~ 60 times lower than for the case $B = 0.15\mu G$.

The ICS contribution due to secondary electrons is not time dependent and is therefore present even if the merger occurred at the epoch of the cluster formation. If the primary electrons are responsible for the hard X-ray excess, then we have to be in a quite narrow window of times after the merger, otherwise the contribution fades away due to electron energy losses. The possible small excess at energies below ~ 1 keV is not appreciably time dependent. This is due to the fact that the cooling time for the low energy electrons is relatively long. One comment that is probably worth making is the following: if one compares the results in Figs. 1 and 2, it is possible to note that, for instance 5×10^8 yrs after the end of the merger, the radio flux in the region accessible to observations is basically absent, while there is an appreciable X-ray flux below ~ 1 keV and above 20–30 keV. This implies that the detection of an X-ray excess without a corresponding radio excess does not automatically imply an upper limit on the magnetic field. This should be taken into account when an upper limit on the magnetic field of a cluster is derived from

these considerations [36], by imposing that the radio emission is too low to be detected.

Any model for the soft or hard X-ray emission must face the gamma ray limit. The gamma ray emission from a cluster at 100 Mpc is plotted in Fig. 3. The thick solid lines represent the gamma ray fluxes due to pion decay in pp scattering for $\xi = 0.1$ (curve Pion01) and $\xi = 0.01$ (curve Pion001). The three dashed lines represent the gamma ray flux due to bremsstrahlung of the primary electrons at the three different times used in Figs. 1 and 2. The dash-dot-dot-dotted lines are the fluxes of gamma rays due to bremsstrahlung emission of the secondary electrons for $\xi = 0.1$ (curve BS01) and $\xi = 0.01$ (curve BS001). The thin solid lines are the gamma ray fluxes due to ICS of the secondary electrons. The upper curve is for $\xi = 0.01$ (ICS001) and the lower curve is for $\xi = 0.1$ (ICS01). All these cases are referred to eq. (3) as diffusion coefficient but are not appreciably affected by other choices. For the ICS of primary electrons the situation is different: in the diffusion scenario adopted here [eq. (3)] the maximum energy of the primary electrons is too low to generate appreciable gamma ray fluxes in the GeV region. However, for a bohm diffusion [eq. (8)] the maximum energy becomes large enough and the correspondent gamma ray flux is plotted in fig. 3 as a dotted line.

It is easy to recognize the strength of the gamma ray limit. Note that even if the total energy in primary electrons is only $\sim 1 - 3\%$ of the merger energy input, the gamma ray fluxes are comparable with the EGRET sensitivity (for a distance of 100 Mpc). Moreover, if the maximum energy of the primary electrons is larger than ~ 200 GeV, a large gamma ray flux is produced by ICS.

Another feature which is evident from Fig. 3 is that while the gamma ray fluxes at energies above ~ 1 GeV contributed by primary electrons fastly fade away, the contribution of gamma rays from pion decay and ICS of secondary electrons remains important. Actually, as proposed in [10], the flux of gamma rays above 10 – 100 GeV can be used as a direct tool to weigh the cosmic ray energy content of clusters. This is due to the fact that *a)* protons do not lose energy appreciably, *b)* the spectrum of the gamma rays from pion decay follows the same spectrum of the parent protons at high energy, *c)* the spectrum of electrons and therefore also the spectrum of the bremsstrahlung emission, is steepened by the electron energy losses, so that their contribution at high energy is negligible.

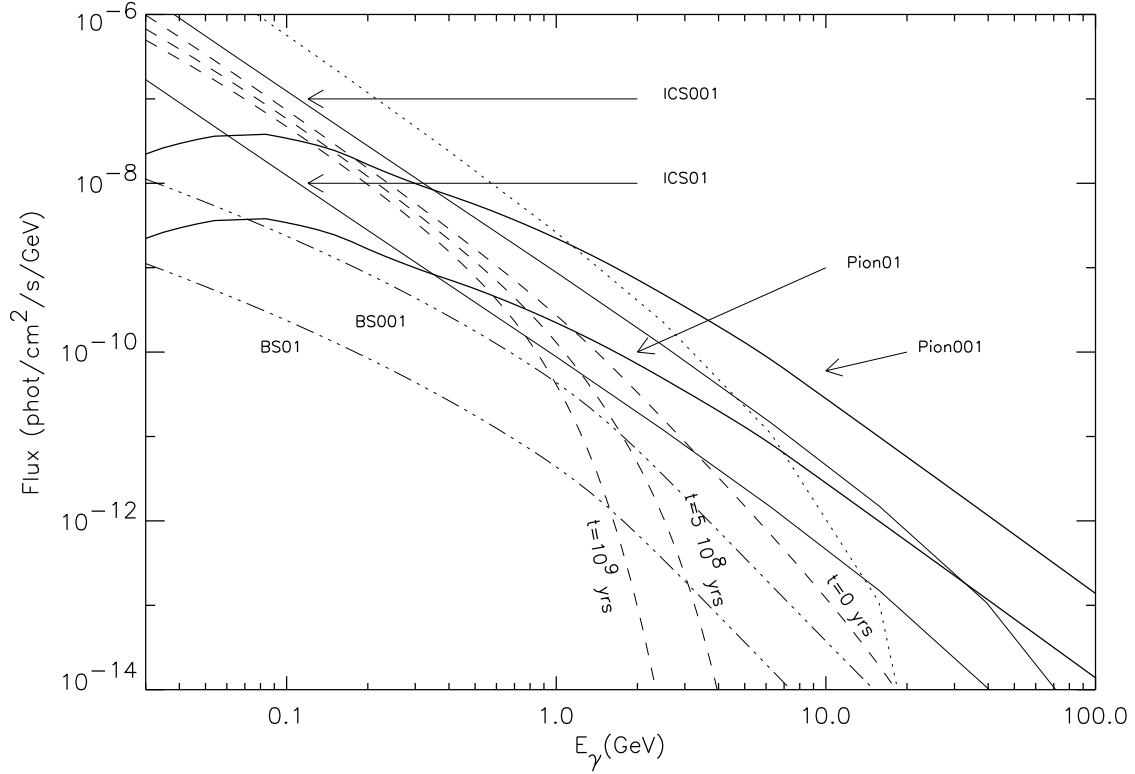


Fig. 3. *Gamma ray fluxes from a cluster at 100 Mpc distance. The dashed lines are the bremsstrahlung contribution from primary electrons at different times after the merger, the thick solid lines represent the gamma rays from pion decay for $\xi = 0.1$ (curve Pion01) and $\xi = 0.01$ (curve Pion001), the dash-dot-dot-dotted lines represent the bremsstrahlung emission from secondary electrons for $\xi = 0.1$ (curve BS01) and $\xi = 0.01$ (curve BS001). The thin solid lines represent the ICS contribution from secondary electrons for $\xi = 0.1$ (curve ICS01) and $\xi = 0.01$ (ICS001). The dotted line is the ICS gamma ray flux from primary electrons at $t = 0$ for a Bohm diffusion coefficient. At later times this contribution rapidly fades away.*

6 The case of the Coma cluster

As an application of the calculations illustrated above, we present the case of the Coma cluster, where excesses in UV and X-rays are detected, as well as a radio halo extended up to frequencies of a few GHz. In the merger model this situation can be realized if the merger has just occurred, and indeed there are some indications that this might be the case for Coma.

If Fig. 4 we plotted the results of our calculations for the radio emission, on top of the data points obtained in [37]. The (solid) line that fits the data is the contribution of the primary electrons with an injection rate correspondent to $\sim 2\%$ of the total luminosity of the merger L_{merger} when the magnetic

field is $0.15\mu G$. The dash-dotted line represents the case $B = 1\mu G$, in which only 0.03% of L_{merger} is needed to explain the radio observations. L_{merger} has been estimated as the ratio of the total thermal energy in the cluster within 1 Mpc from the center, and the merger duration ($\sim 10^9$ yrs). The number we obtained can be considered as an upper limit, since the gas was presumably already hot before the merger. The diffusion coefficient was chosen as in eq. (3) with $v_8 \approx 4.8$ and $L_{20} \approx 10$ (200 kpc, correspondent to the typical distance between two galaxies in Coma). These values were chosen only in order to obtain a maximum energy for the primary electrons large enough to generate GHz radio waves. In the case of Bohm diffusion this problem does not appear, but there is no cutoff at GHz frequencies (see fig. 1).

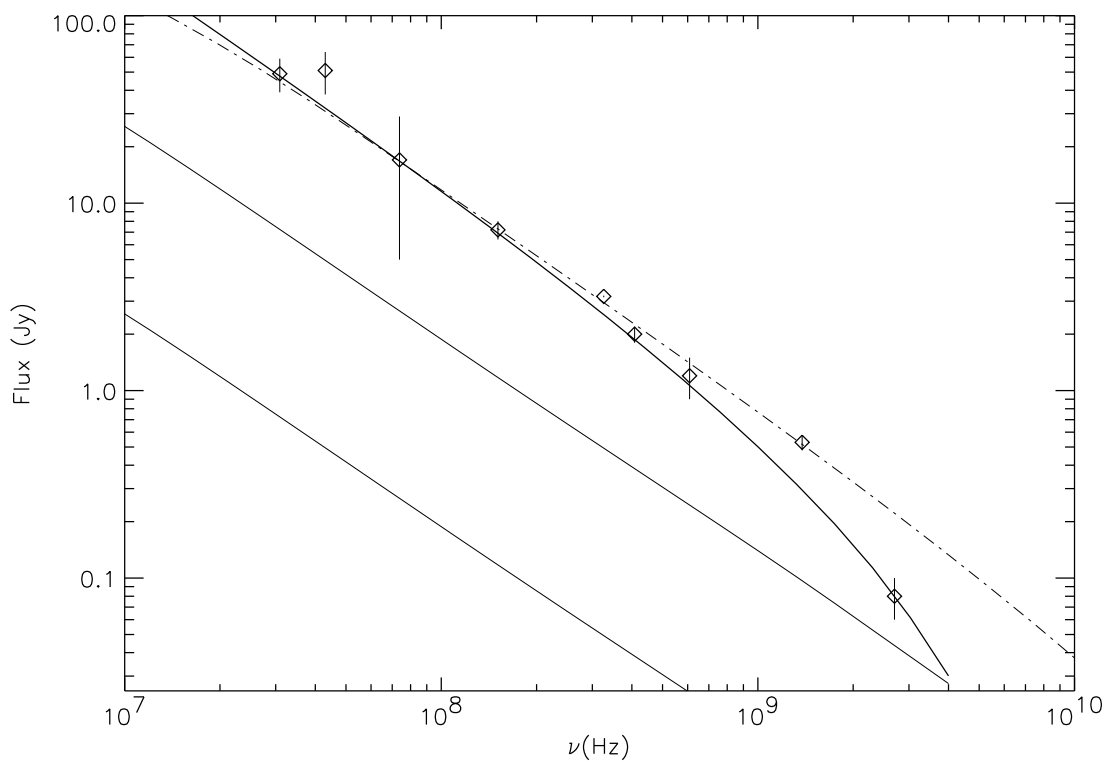


Fig. 4. Radio emission from the Coma cluster. The data points from [37] are well fitted by the primary electron synchrotron emission for $B = 0.15\mu G$. The other two solid curves represent the contribution of secondary electrons for $\xi = 0.1$ (lower curve) and $\xi = 0.01$ (upper curve), again for $B = 0.15\mu G$. The dash-dotted line is the synchrotron flux from primary electrons for $B = 1\mu G$.

The two bottom lines in Fig. 4 are the contribution of the secondary electrons for $\xi = 0.1$ (correspondent to $\sim 5\%$ of L_{merger}) and $\xi = 0.01$ (corresponding to $\sim 46\%$ of L_{merger}).

The corresponding ICS contributions to UV and soft/hard X-rays are plotted in Fig. 5, together with the thermal contribution from a gas at the temperature

of Coma (thick solid line). The data points are from Beppo-SAX, while the dark region is an estimate of the soft X-ray/UV flux [38]. The thin solid line is the ICS contribution of primary electrons for $B = 0.15\mu G$: both the UV and hard X-rays are quite well described by this curve. The two dashed lines are the ICS fluxes of secondary electrons for $\xi = 0.1$ (lower curve) and $\xi = 0.01$ (upper curve). The dash-dotted line is the ICS flux from primary electrons for $B = 1\mu G$. It is evident that in this case the relativistic electrons give a negligible contribution to the X-ray flux, therefore, for the large fields found by Faraday rotation measurements, ICS cannot be invoked as an explanation of the hard X-ray excess. For fields even higher than $1\mu G$ clearly the problem becomes more evident.

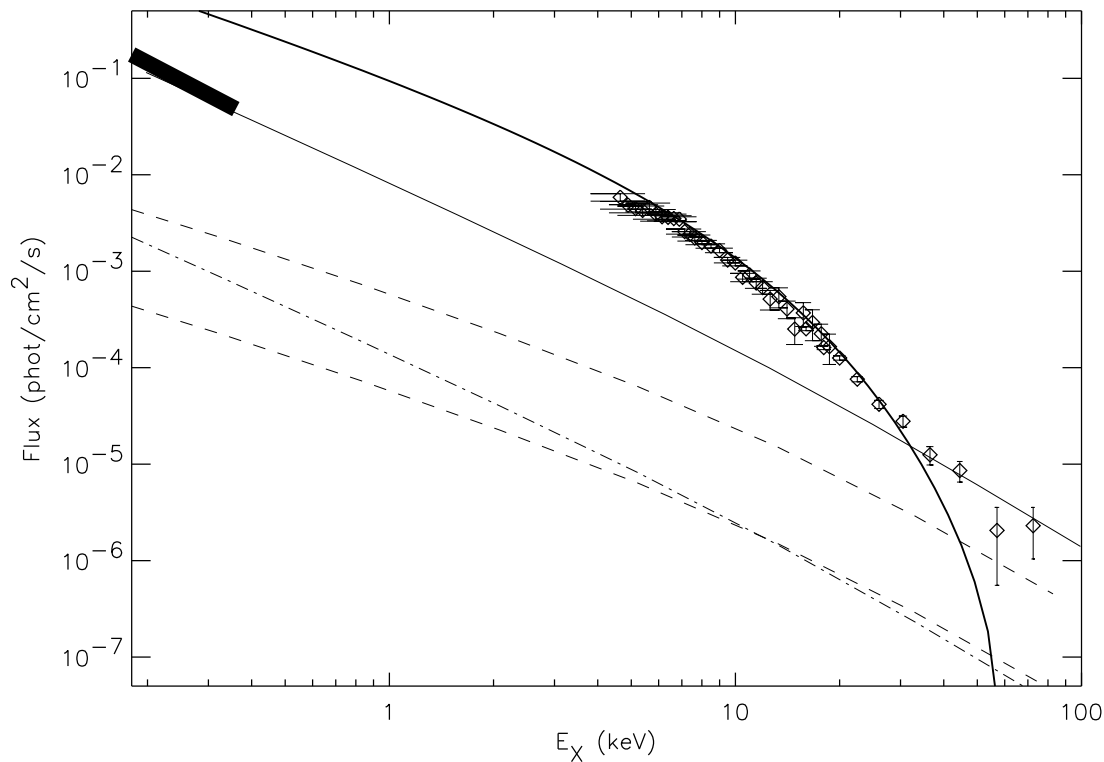


Fig. 5. X-ray emission from the Coma cluster. The data points are from [2]. The solid thick line is the bremsstrahlung emission of thermal gas, the solid thin line is the ICS flux from primary electrons, and the two dashed lines are the ICS fluxes from secondary electrons for the two usual values of ξ and $B = 0.15\mu G$. The dark region is an estimate of the low energy X-ray excess from [38]. The dash-dotted line is the X-ray flux expected from primary electrons for $B = 1\mu G$, too small by a factor ~ 60 .

Is the low magnetic field situation compatible with the gamma ray bound? In Fig. 6 we plotted the gamma ray flux from Coma, separating the contribution of the bremsstrahlung from the primary electrons (thick line) and secondary electrons (dash-dotted lines), the pion decay for the usual two values of the

parameter ξ (thin solid lines) and the ICS of the secondary electrons (dashed lines). The dotted line represents the ICS flux from primary electrons when a Bohm diffusion is used. In the other case, for the reasons explained above there is no gamma ray flux due to ICS of primary electrons. The gamma ray flux at ~ 100 MeV exceeds the EGRET upper limit [39] by a factor $\sim 2-4$ for the diffusion coefficient in eq. (3) and by a factor ~ 15 for the Bohm diffusion.

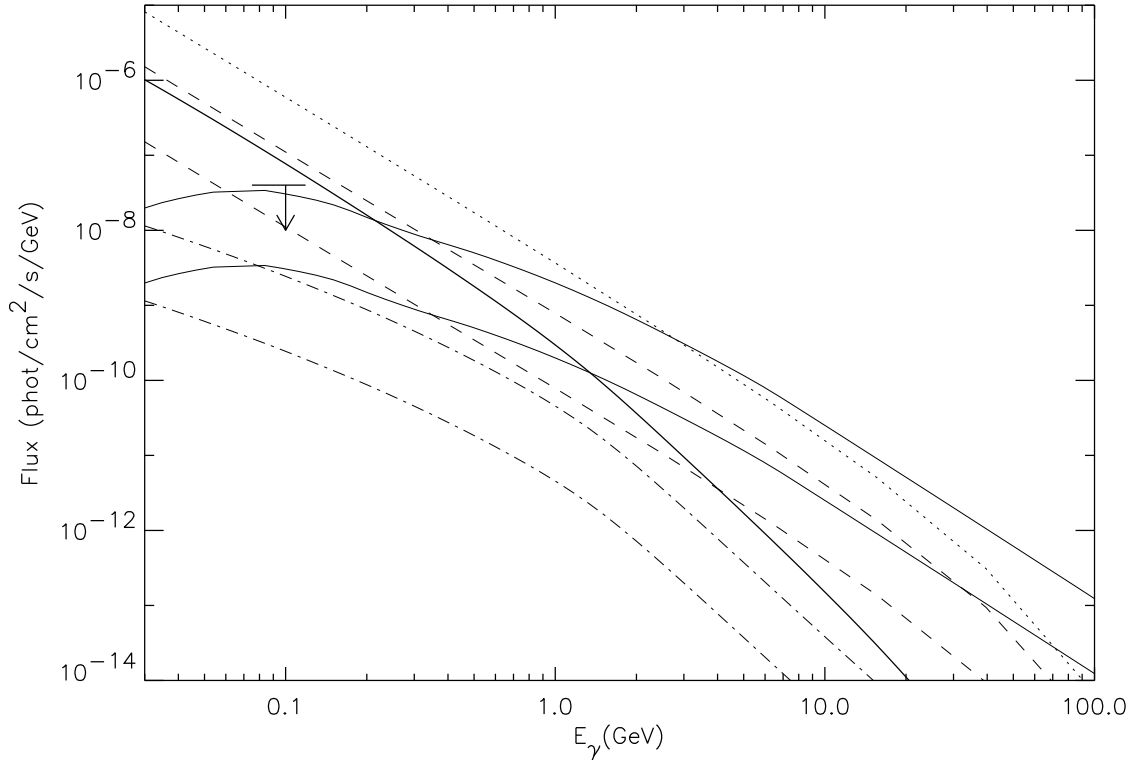


Fig. 6. *Gamma ray fluxes from the Coma cluster. The EGRET upper limit is from [39]. The solid thin lines are the result of pion production for $\xi = 0.1$ (lower curve) and $\xi = 0.01$ (upper curve). The solid thick line is the bremsstrahlung contribution of primary electrons. The dashed lines are the ICS fluxes from secondary electrons for $\xi = 0.1$ (lower curve) and $\xi = 0.01$ (upper curve). The dotted line is the ICS gamma ray flux from primary electrons in the case of Bohm diffusion.*

The estimate of the gamma ray excess at 100 MeV may be affected by the assumptions on the spatial distribution of the injected cosmic rays, but it is difficult to envision how to reduce the predicted flux in such a way that the results become compatible with the EGRET limit. It is worth to stress again the role of current and future gamma ray detectors to clarify the origin of the non-thermal radiation from clusters of galaxies, as already discussed in [10]: if the flux of gamma rays from Coma is just below the EGRET upper limit, additional efforts for its detection would certainly help in understanding the source of the radiation at other wavelengths.

7 Discussion and Conclusions

The role of mergers of clusters of galaxies for the heating of the intracluster gas has already been recognized through observations as well as through numerical simulations. The heating mainly occurs due to the formation of collisionless shocks, whose presence shows up in simulations and in observations through the appearance of hot rims. Being the typical compression factor of these shocks in the range $r \sim 3 - 4$, they may be of some relevance for the acceleration of a fraction of the thermal gas to ultra-relativistic energies, by first order Fermi acceleration.

We studied here the non-thermal radiation generated by electrons and protons energized at a typical merger shock in a generic cluster. The aim of this calculation was not to consider a specific case, but rather to draw some general conclusions about the role of mergers as sources of the non-thermal radiation recently detected from several clusters of galaxies.

The main problem with reaching this goal is that mergers are short events on cosmological time scales, but relatively long duration events on the scale of energy losses of electrons in the CMB bath. Therefore, whether a merger can induce or not an appreciable flux of non-thermal radiation through ICS and synchrotron emission of high energy electrons depends on how long ago the cluster merger occurred, in terms of acceleration of new particles. This is not true for the secondary electron component, generated through the decay of charged pions in pp interactions. Due to the confinement of cosmic ray protons in the cluster [11], the contribution to the non-thermal radiation, due to secondary electrons is basically time independent after the end of the merger event.

A possible summary of the results obtained here is as follows:

i) As shown in Fig. 1, the radio emission due to primary electrons is dramatically time dependent. If the injection of newly accelerated particles ends (the merger is over), after 5×10^8 yrs the radio emission above ~ 30 MHz has already disappeared. The radio emission due to secondary electrons is a function of the ratio of protons to electrons, but, as illustrated in Fig. 1, this contribution is appreciable for a cluster at a typical distance of 100 Mpc. As stated before, this emission is time independent, therefore, if a diffuse radio emission is detected in a cluster where there is no current evidence of a very recent merger, this would indicate the presence of a substantial relativistic hadronic component in the intracluster medium.

ii) As far as the X-ray emission is concerned, it is quite well proven that the bulk of the X-ray radiation from clusters of galaxies is due to bremsstrahlung of thermal electrons at a temperature of $10^7 - 10^8$ K. The soft and hard X-

ray and the extreme UV excesses recently detected from some clusters need further investigation: for the UV excess, there seem to be different tendencies, from a thermal interpretation [8,9] to a ICS interpretation [40,6]. In the hard X-ray region the evidence for an excess seems to be more solid. In Fig. 2 we plotted the ICS contribution in the region of interest, by dashed lines (for $B = 0.15\mu G$). Although after 5×10^8 yrs the X-ray flux above ~ 30 keV is considerably reduced, it seems still appreciable, while, as stated above, the correspondent radio flux above 30 MHz has faded away. This means that there is a time window where there might be X-ray activity and no radio flux. In this case it is not possible to extract upper limits on the magnetic field from the absence of radio emission. The dash-dotted line refers to the case $B = 1\mu G$ and makes clear that large magnetic fields considerably decrease the amount of non-thermal X-ray emission.

The X-ray flux generated by ICS of secondary electrons may be appreciable, and, as for the radio flux, it is time independent, so that it is still present even when the whole contribution from primary electrons has disappeared. Fig. 2 also makes clear that it is more promising to look for non-thermal excesses in lower temperature clusters, where the contribution due to thermal bremsstrahlung disappears at lower energies, leaving the hard X-ray fluxes to dominate.

iii) What is the overall energy requirement in order to have reasonably large non-thermal fluxes and how large can the magnetic field be? We found that a few percent of L_{merger} in the form of accelerated electrons can explain the observations if the merger is very recent (see for instance the case of Coma in section 6). This issue is directly related to the strength of the magnetic field in the ICM. This is an open issue: it is not easy to envision a simple reason why Faraday rotation measurements (that always provide a result smaller than the “real” field) actually give values higher or even much higher [3,4] than the field required to explain the multiwavelength observations of clusters. At present there is no theoretical argument that may help in estimating the value of the magnetic field in clusters, since its origin is a complete mystery. The intracluster field might be cosmological [41], or might as well be generated in shock waves during the process of formation of large scale structures [42] or expelled by radio galaxies [43,44] or by galactic winds [45,46]. In any case the theoretical input on this issue is not significant and the main source of information on the magnetic field is either through indirect measurements (radio plus X-rays) or by measurements of the Faraday rotation, and as we stressed above, these two methods give results which do not seem compatible with each other.

The need for small magnetic fields is common to all models based on ICS (for the hard X-rays) and synchrotron (for the radio emission) and is not limited to cluster merger scenarios. This seems to us as a strong argument against this

class of models, that should stimulate the search for alternative explanations. The problem is evident from Figs. 1 and 2: the dash-dotted lines are the non-thermal fluxes for the case $B = 1\mu G$; the radio emission can be at the same level as in the case $B = 0.15\mu G$, with about 60 times less electrons, but the X-ray fluxes are correspondingly lower by a factor 60.

Is there any way to reconcile the results of Faraday rotation measurements with the magnetic field required by non-thermal observations? One possibility is that regions of very high magnetic field are separated by regions where the magnetic field is lower. In these conditions the Faraday rotation might be affected mainly by the strongly magnetized regions while the hard X-rays would come from the low field regions. This scenario might imply a phase separation in the intracluster medium, which is actually observed in some cases (see for instance [47]). However such a situation does not seem to be happening in clusters like Coma or other clusters that show non-thermal activity and appear relaxed. Moreover, the flux of hard X-rays is basically independent of the magnetic field (it is the normalization between X-rays and radio emission that implies low magnetic fields), therefore the large gamma ray fluxes studied in section 6 would not be affected by this argument, and in the case of the Coma cluster the predicted gamma ray fluxes would still be in excess of the EGRET upper limit.

For this reason gamma ray observations can be considered as a more solid constraint on the total amount of energy that can be injected in the cluster (therefore indirectly also on the strength of the average magnetic field). Gamma ray emission in a cluster is produced mainly by a) bremsstrahlung emission of primary and secondary electrons, b) ICS of primary and secondary electrons, and c) decay of neutral pions generated in pp interactions. The results are plotted in Fig. 3: the bremsstrahlung of primary electrons fades away quite rapidly, but it remains important below a few hundreds MeV, accessible to EGRET. The bremsstrahlung of the secondary electrons is usually quite small. A very important contribution to the gamma ray emission is provided by ICS of the secondary electrons. It is worth recalling again that this flux is not time dependent, therefore it does not fade away with time, even if the merger occurred in the distant past of the cluster. The same is true for the gamma ray emission due to pion decay. The ICS contribution of primary electrons depends on the maximum energy of the electrons, which is in turn affected by the choice of the diffusion coefficient.

To make the prediction more quantitative, we applied our calculations to the case of the Coma cluster. For a merger that just ended, the radio flux can be fitted quite well by the synchrotron emission of primary electrons. The results are plotted in Fig. 4. The cut off at a few GHz is here the result of a cutoff in the spectrum of the accelerated electrons and it could be absent for a different model of diffusion (the existence of the cutoff in the observations

has been questioned anyway in [48]). The value of the magnetic field required to fit simultaneously the radio and hard X-ray emission is $B = 0.15\mu G$ for an emission volume of 1 Mpc. With these parameters the soft X-ray and UV excesses are also of the correct order of magnitude. A larger field of $B = 1\mu G$ is used to obtain the dash-dotted line, corresponding to a rate of injection of electrons ~ 60 times lower than in the previous case. For $B = 1\mu G$ the X-ray flux by ICS is ~ 60 times too small to explain the BeppoSAX observations (Fig. 5).

What is the role of protons in the Coma cluster? With the parameters used above, the contribution of secondary electrons to both radio and hard X-ray emission is small, but for $\xi = 0.01$ the EGRET upper limit to the gamma ray flux above 100 MeV is saturated. Indeed this limit is exceeded by the bremsstrahlung of primary electrons added to the ICS emission of secondary electrons (Fig. 6) and possibly of primary electrons (if their maximum energy is large enough).

What happens if the merger occurred more than, say, 10^9 yrs ago? In this case, as discussed above, the contribution of primary electrons has become negligible by now, therefore the secondary electrons must be responsible. From Figs. 4-6 we see that this implies a large energy injection in cosmic ray protons, resulting in a flux of gamma radiation with energy larger than 100 MeV which is in excess of the EGRET limit. Even if the merger occurred very recently the gamma ray fluxes are close to or even in excess of the EGRET upper limit.

From the discussion above, it is clear that the interpretation of the non-thermal multiwavelength observations from clusters (and in particular from Coma) based on synchrotron and ICS of relativistic electrons has several severe problems. Therefore it is natural to look for some alternative explanations. We address this issue briefly: is it possible that mergers play a role in the production of non-thermal radiation and, at the same time, that intracluster magnetic fields are at the level measured through Faraday rotation keeping the gamma ray fluxes below the EGRET upper limit? As we showed, if ICS and synchrotron emissions are used as mechanisms for the production of the non-thermal radiation, then the answer is likely to be negative. However, in [5] a viable alternative was presented: during the merger the perturbation of the magnetic field results in the production of waves that can resonate with electrons on the tail of the thermal electron distribution. Since waves and electrons are coupled non-linearly, part of the energy released in the tail of the Maxwell-Boltzmann distribution ends up in the low energy part of the electron spectrum and is rapidly redistributed in the form of thermal energy of the plasma. In other words, it was shown that the thermalization process in the presence of a magnetic field and a perturbation (e.g. the merger) is not a simple process, and while the bulk of the thermal electrons is “just” heated up, the fraction of electrons more weakly bound to the thermal bath can acquire

a non-Maxwellian distribution. If this happens, then the hard X-rays can be the result of bremsstrahlung emission of the non-thermal tail [5–7], without affecting at all the radio emission, that can be generated through synchrotron radiation of a population of electrons radiating in a magnetic field consistent with Faraday rotations. The gamma ray fluxes would also be insignificant. This scenario has two nice features: 1) it provides a unified picture for the heating process and for the energization of low energy electrons to non-thermal energies; 2) it explains the thermal and non-thermal X-ray emission in terms of the same process (bremsstrahlung emission).

In [49] it was proposed a clear way of testing this scenario, by using precision measurements of the Sunyaev-Zeldovich effect from clusters of galaxies showing non-thermal activity.

Acknowledgments I am grateful to C. Sarazin and P.L. Biermann for discussions. I am also grateful to R. Fusco-Femiano for kindly providing the BeppoSAX data of the X-ray emission from the Coma cluster and to the anonymous referee for useful comments. This work was supported by the DOE and the NASA grant NAG 5-7092 at Fermilab.

References

- [1] T.A. Ensslin, in the Proceedings of *The Universe at Low Radio Frequencies*, ASP Conference Series, 1999 (preprint astro-ph/0001433).
- [2] R. Fusco-Femiano, D. Dal Fiume, L. Feretti, G. Giovannini, P. Grandi, G. Matt, S. Molendi, A. Santangelo, *Astrophys. J.* 513 (1999) L21.
- [3] J.A. Eilek, preprint astro-ph/9906485, to appear in 'Diffuse Thermal and Relativistic Plasma in Galaxy Clusters', 1999, Ringberg Workshop, Germany, MPE-Report.
- [4] T.E. Clarke, P.P. Kronberg, H. Böhringer, in Ringberg Workshop on "Diffuse Thermal and Relativistic Plasma in Galaxy Clusters", Eds: H. Böhringer, L. Feretti, P. Schuecker, MPE Report No. 271, 1999.
- [5] P. Blasi, *Astrophys. J. Lett.* 532 (2000) L9.
- [6] T.A. Ensslin, R. Lieu, P. Biermann, *A&A* 344 (1999) 409.
- [7] V.A. Dogiel, in Ringberg Workshop on "Diffuse Thermal and Relativistic Plasma in Galaxy Clusters", Eds: H. Böhringer, L. Feretti, P. Schuecker, MPE Report No. 271, 1999.
- [8] M. Bonamente, R. Lieu, preprint astro-ph/0001128.
- [9] R. Lieu, M. Bonamente, J.P.D. Mittaz, preprint astro-ph/0001127.

- [10] P. Blasi, *Astrophys. J.* 525 (1999) 603.
- [11] V.S. Berezhinsky, P. Blasi, V.S. Ptuskin, *Astrophys. J.* 487 (1997) 529.
- [12] T.A. Ensslin, P.L. Biermann, *A&A* 330 (1998) 90.
- [13] H.J. Volk, F.A. Aharonian, D. Breitschwerdt, *Space Sci. Rev.* 75 (1996) 279.
- [14] T.A. Ensslin, P.L. Biermann, P.P. Kronberg, X.-P. Wu, *Astrophys. J.* 477 (1997) 560.
- [15] C.L. Sarazin, To appear in *Large Scale Structure in the X-ray Universe*, edited by M. Plionis and I. Georgantopoulos (Paris: Editions Frontieres), in press (preprint astro-ph/9911439).
- [16] R. Blandford, D. Eichler, *Phys. Rep.* 154 (1987) 1.
- [17] K. Roettiger, J. Stone, R. Mushotzky, *Astrophys. J.* 493 (1998) 62.
- [18] K. Roettiger, J. Stone, J.O. Burns, *Astrophys. J.* 518 (1999) 594.
- [19] P.M. Ricker, *Astrophys. J.* 496 (1998) 670.
- [20] D.S. Krivitsky, V.M. Kontorovich, *A&A* 327 (1997) 921.
- [21] K. Roettiger, C. Loken, J.O. Burns, *Astrophys. J. Suppl.* 109 (1997) 307.
- [22] M. Takizawa, T. Naito, preprint astro-ph/0001046 (accepted for publication in *Astrophys. J.*).
- [23] P. Blasi, S. Colafrancesco, *Astropart. Phys.* 12 (1999) 169.
- [24] K.G. McClements, R.O. Dendy, R. Bingham, J.G. Kirk, L. O’C. Drury, *MNRAS* 291 (1997) 241.
- [25] A. Levinson, *Astrophys. J.* 426 (1994) 327.
- [26] A.R. Bell, *MNRAS*, 182 (1978) 443.
- [27] A.R. Bell, *MNRAS*, 182 (1978) 147.
- [28] C.L. Sarazin, *X-ray Emission from Clusters of Galaxies* (Cambridge Univ. Press, Cambridge, 1988).
- [29] F.W. Stecker, *Astrophys. J.* 228 (1979) 919.
- [30] C.D. Dermer, *A&As* 157 (1986) 223.
- [31] A.W. Strong and I.V. Moskalenko, *Astrophys. J.* 493 (1998) 694.
- [32] C.L. Sarazin, *Astrophys. J.* 520 (1999) 529.
- [33] M. Markevitch, C.L. Sarazin, A. Vikhlinin, *Astrophys. J.* 521 (1999) 526.
- [34] S. Colafrancesco, P. Blasi, *Astropart. Phys.* 9 (1998) 227.
- [35] J.R. Jokipii, *Astrophys. J.* 313 (1987) 842.

- [36] J.C. Kempner, C.L. Sarazin, *Astrophys. J.* 530 (2000) 282.
- [37] L. Feretti, D. Dallacasa, G. Giovannini, A. Tagliani, *A&A* 302 (1995) 680.
- [38] R. Lieu, R., W.-H. Ip, W.I. Axford, M. Bonamente, *Astrophys. J.* 510 (1999) 25.
- [39] P. Sreekumar et al., *Astrophys. J.* 464 (1996) 628.
- [40] C.L. Sarazin, R. Lieu, *Astrophys. J.* 494 (1998) 177.
- [41] A.V. Olinto, 1997, in 3rd RESCEU International Symposium on “Particle Cosmology”, University of Tokyo, astro-ph/9807051.
- [42] H. Kang, J.P. Rachen, P.L. Biermann, *MNRAS* 286 (1997) 257.
- [43] R.A. Daly, A. Loeb, *Astrophys. J.* 364 (1990) 451.
- [44] S.E. Okoye, L.I. Onuora, *MNRAS* 283 (1996) 1047.
- [45] P.P. Kronberg, H. Lesch, U. Hopp, *Astrophys. J.* 511 (1999) 56.
- [46] H.J. Völk, A.M. Atoyan, in Ringberg Workshop on “Diffuse Thermal and Relativistic Plasma in Galaxy Clusters”, Eds: H. Böringer, L. Feretti, P. Schuecker, MPE Report No. 271, 1999.
- [47] B.R. McNamara, W. Wise, P.E. Nulsen, L.P. David, C.L. Sarazin, M. Bautz, M. Markevitch, A. Vikhlinin, W.R. Forman, C. Jones, D.E. Harris, submitted to *Astrophys. J.*
- [48] R.M. Deiss, W. Reich, H. Lesch and R. Wielebinski, *A&A* 321 (1997) 55.
- [49] P. Blasi, A.V. Olinto, A. Stebbins, *Astrophys. J. Lett.* (2000) in press.